Adsorption (2007) 13: 515–522
DOI 10.1007/s10450-007-9063-z

Liquid-phase adsorption experiments on ordered mesoporous silicas

R. Rockmann · G. Kalies · O. Klepel

Received: 29 April 2007 / Revised: 29 April 2007 / Accepted: 24 September 2007 / Published online: 18 October 2007

Abstract SBA-15, SBA-16 and MCM-48 silicas with hexagonal $p\bar{6}mm$, cubic $Im\bar{3}m$ and cubic $Ia\bar{3}d$ mesopore structure were synthesized according to known methods reported in literature and characterized by X-ray diffraction and nitrogen adsorption. Liquid-phase adsorption experiments were performed on all three materials. The adsorption behavior of binary liquid model mixtures was studied over the whole concentration range with regard to the separation quality of the solid and the dependence on the chain length of adsorptive molecules. Inverted U-shape isotherms were found indicating that the silicas are highly selective for polar components. So far, an influence of mesopore size or structure on liquid excess isotherms cannot be extracted from the measured data. The present work is a first step to create a data base of liquid-phase adsorption on solids with ordered mesopore structure.

Keywords Liquid-phase adsorption · Excess isotherms · Binary liquid mixtures · Chain length · Ordered mesoporous silicas · Gas adsorption

R. Rockmann
Wilhelm Ostwald Institute of Physical and Theoretical Chemistry, University of Leipzig, 2 Linnéstrasse, 04103 Leipzig, Germany

G. Kalies (✉)
Institute of Experimental Physics I, University of Leipzig, 5 Linnéstrasse, 04103 Leipzig, Germany
e-mail: kalies@uni-leipzig.de

O. Klepel
Institute of Technical Chemistry, University of Leipzig, 3 Linnéstrasse, 04103 Leipzig, Germany

Abbreviations

$\Gamma_i^{(n)}$	adsorption excess of component i, related to the mass of solid (mmol/g) or to the BET specific surface area of solid (μmol/m^2) or to the total pore volume of solid (mmol/cm^3)
$n_2^{\sigma(n)}$	excess amount of component 2, mmol
n^0	total amount of component 1 and 2 in the original mixture, mmol
x_2^0	mole fraction of component 2 before adsorption
x_2	mole fraction of component 2 in adsorption equilibrium
m_A	mass of adsorbent, g
$\Gamma_2^s, h_1, U_1, U_2$	parameters of the Bi-Langmuir function (Bräuer et al. 2002)
T	temperature, K
R	gas constant, 8.314472 J/(mol K)
S_{BET}	BET specific surface area, m^2/g
V_t	total pore volume, cm^3/g
V_{mi}	micropore volume, cm^3/g
d_{me}	average mesopore diameter, Å

1 Introduction

In recent years, extensive work has been reported on synthesis and characterization of solids with ordered mesopore structure (Zhao et al. 1998a, 1998b; Kruk et al. 2000; Wang et al. 2001; Choi et al. 2003; Kim et al. 2005; Kleitz et al. 2005). Beside other methods, physical gas adsorption is widely used for the textural characterization of mesoporous solids (Thommes 2004). The number of papers concerning liquid adsorption on mesoporous solids over the

whole concentration range is strongly limited as liquid adsorption is not used as standard method for characterizing solids (Rockmann and Kalies 2007). The basic problem in interpretation and utilization of liquid adsorption experiments lies in the fact that, in contrast to pure gas adsorption, primary measurable information is given by adsorption excess isotherms of binary mixtures. As can be easily understood, the measurable liquid adsorption excess is dependent on solid qualities (porosity, structure, surface area, chemical composition etc.), liquid qualities (nature of adsorptives, mixture behavior, concentration etc.), pressure and temperature, i.e., the variety of quantities influencing size and shape of isotherms is, compared to that of gas adsorption, increased by the mixture behavior in the bulk liquid and in the vicinity of the solid surface. Nevertheless, thermodynamics provides a useful tool for obtaining relevant information from binary liquid-phase adsorption on solids, e.g.:

(1) Information on the separation and mixture behavior of binary and multicomponent liquid mixtures at different interfaces by means of the absolute formalism (Everett 1986; Kalies et al. 2000a).
(2) Information on the adsorption excesses of multicomponent liquid mixtures at different interfaces by means of the absolute or excess formalisms (Myers et al. 1987; Price and Danner 1987; Kalies et al. 2000b; Bräuer et al. 2002; Kalies and Bräuer 2005).
(3) Information on the immersion behavior of binary and multicomponent liquid mixtures on solid surfaces (Kalies et al. 2005).
(4) Information on the heterogeneity of the solid adsorbent by solving the adsorption integral equation (Heuchel et al. 1993).

The purpose of this paper is to present recent experimental results in liquid-phase adsorption on mesoporous silicas of the newer generation. On the one hand, the materials exhibit high pore volumes and surface areas, and their surfaces can by easily functionalized, i.e. they promise application in catalysis, separation, pollutant removal etc. On the other hand, solids with tunable mesopore sizes and uniform pore structure can be used as model adsorbents to test and develop theories of liquid-phase adsorption. As many experimental liquid adsorption excess isotherms are presented, data interpretation according to point 1–4 will be given in further papers. The work contributes to application research of mesoporous solids and to the study of liquid-phase adsorption in mesostructures.

2 Theory

The primary experimental quantity in liquid adsorption is the adsorption excess or so-called reduced adsorption of component 2 of a binary liquid mixture, denoted by $\Gamma_2^{(n)}$ (IUPAC 1993). It is defined as:

$$\Gamma_2^{(n)} = \frac{n_2^{\sigma(n)}}{m_A} = \frac{n^0}{m_A}(x_2^0 - x_2); \qquad \Gamma_2^{(n)} = -\Gamma_1^{(n)}, \tag{1}$$

$n_2^{\sigma(n)}$ being the excess amount of component 2, n^0 the total amount of component 1 and 2 in the original mixture and $x_2^0 - x_2$ the change in mole fraction of the bulk liquid caused by adsorption on an adsorbent of the mass m_A.

The measured $\Gamma_2^{(n)}(x_2)$ excess isotherms as a function of the mole fraction of the preferentially adsorbed component 2 can be described by different functions such as the Bi-Langmuir function (Bräuer et al. 2002)

$$\Gamma_2^{(n)} = \Gamma_2^s \left(h_1 \frac{K_1 y}{1 + K_1 y} + (1 - h_1) \frac{K_2 y}{1 + K_2 y} - x_2 \right);$$
$$K_i = e^{\frac{U_i}{RT}}; \quad i = 1, 2; \quad y = \frac{x_2}{1 - x_2}. \tag{2}$$

In order to discuss the measured adsorption excess isotherms, it can be useful to convert the specific adsorption excess (mmol/g) of (1) into an areal adsorption excess (μmol/m^2) or an adsorption excess per unit volume (mmol/cm^3) by means of the specific surface area or the pore volume of the solid adsorbent known from gas adsorption. Since the aim of this paper is mainly liquid-adsorption data presentation and discussion, we will refrain at this point from the presentation of known thermodynamic methods for evaluating liquid adsorption isotherms (Everett 1986; Myers et al. 1987; Price and Danner 1987; Heuchel et al. 1993; Bräuer et al. 2002; Kalies and Bräuer 2005; Kalies et al. 2005 etc.).

3 Experimental

3.1 Materials

The synthesis procedures for the SBA-15, SBA-16 and MCM-48 silica materials used for liquid-phase adsorption experiments are already described in our earlier paper (Rockmann and Kalies 2007). The SBA-15 sample was prepared in a conventional manner using Pluronic P123 (Aldrich) according to the method reported by Zhao et al. (1998a, 1998b). SBA-16 synthesis was performed in analogy to that of SBA-15 but using a mixture of two technical triblock copolymers (Pluronic P123, Pluronic F127, Aldrich) as structure-directing agents (Kim et al. 2005). Last but not least, MCM-48 was synthesized according to the method reported by Wang et al. (2001). Synthesis yields were about 2–3 g. In order to obtain silica quantities sufficiently large for performing liquid-adsorption experiments, the synthesis procedures were repeated, and products with a

comparable degree of order and pore size distribution were merged.

The liquid adsorptives n-octane (>99.5%, Fluka), ethanol, hexanol and octanol (>99.9%, Merck) were used without being further purified.

3.2 Characterization of silicas

Characterization of all samples was carried out by nitrogen adsorption and X-ray diffraction (XRD). Nitrogen-adsorption measurements were performed at −196 °C on the ASAP 2010 volumetric adsorption analyzer (Micromeritics). Prior to measurements, the samples were outgassed at 150 °C for 24 h in the degas port of the ASAP 2010 or by using SCTA sample-controlled thermal analysis (Sorensen and Rouquérol 2003; Rockmann and Kalies 2007). Powder XRD patterns were recorded on the XRD-7 diffractometer (Seifert) using Cu$K\alpha$ radiation.

3.3 Measurement of liquid adsorption isotherms

Excess-isotherm points were determined by the traditional immersion method (Everett 1986). For each isotherm point, a fresh sample of adsorbent was required. The solid sample, ca. 0.1–0.15 g, was outgassed at 150 °C for 24 h, and then, out of contact with atmosphere, cooled to room temperature and contacted with about 0.8 g of liquid mixture of known mole fractions. The amounts of liquid and adsorbent were gravimetrically measured. After 24 h in a thermostat at 25 ± 0.3 °C, the equilibrium mole fractions of the exceeding liquid mixture were determined refractometrically (immersion refractometer with thermoprisms, Carl Zeiss Jena). The experimental error for each isotherm point is about ±0.03 mmol/g.

For the analysis of an adsorption isotherm of 20 data points over the whole concentration range (duplicate or replicate determination) about 10 g of uniform SBA-15, SBA-16 and MCM-48 samples were required. Since the silicas are fine powders bloating in liquids, an appropriate liquid/solid ratio of 1:6 had to be chosen, which ensure on the one hand measurable mole fraction differences $x_2^0 - x_2$ and on the other hand the retrieval of a sample of bulk liquid sufficient for refractometric analysis.

4 Results and discussion

Figure 1 shows the nitrogen adsorption-desorption isotherms and pore size distribution curves, respectively, for the merged SBA-15, SBA-16 and MCM-48 samples used as adsorbents in liquid-phase adsorption. The type IV isotherms show typical capillary condensation indicative of narrow

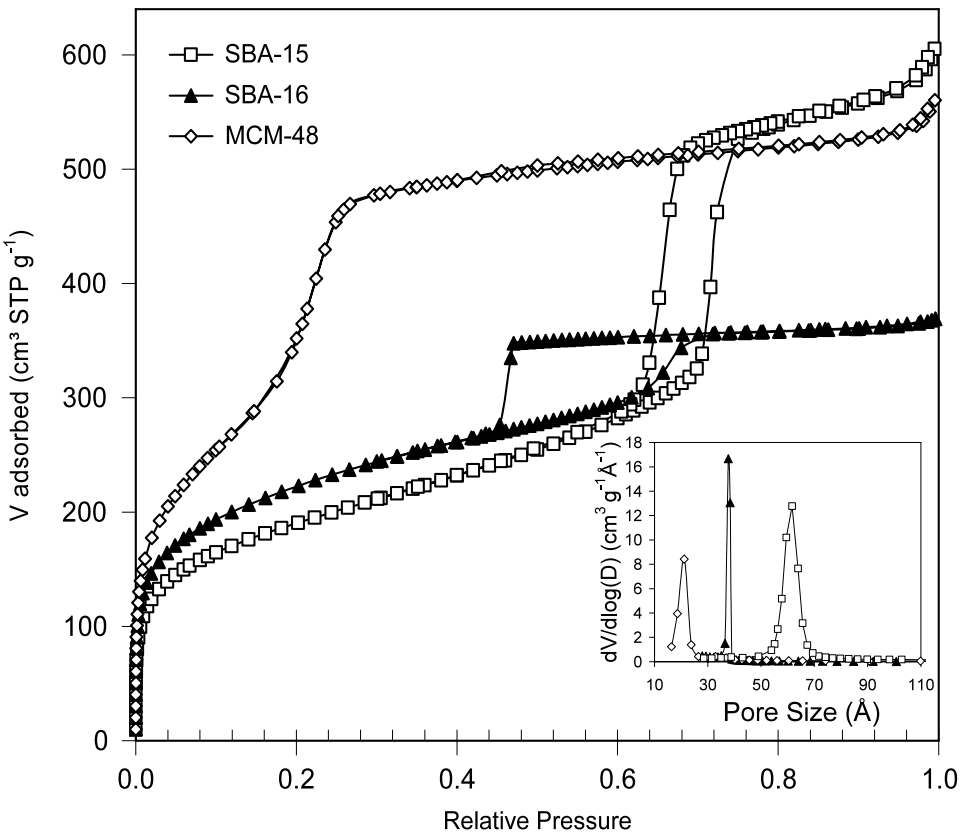

Fig. 1 Nitrogen adsorption-desorption isotherms at −196 °C and BJH pore size distributions (desorption branch) for the merged SBA-15, SBA-16 and MCM-48 silica samples used in liquid adsorption experiments

Table 1 Selected structural parameters of the merged silica samples used as adsorbents in liquid-phase adsorption*

Adsorbent	S_{BET} (m^2/g)	V_t (cm^3/g)	V_{mi} (cm^3/g)	d_{me} (Å)[a]	d_{me} (Å)[d]
SBA-15	690	0.91	0.09	73	61
SBA-16	806	0.57	0.21	60	38
MCM-48	1109	0.83		21	21

* S_{BET}, BET specific surface area; V_t, total pore volume; V_{mi}, micropore volume (t-plot); d_{me}, average mesopore diameter from the BJH mesopore size distribution ([a]calculated from the **a**dsorption branch, [d]calculated from the **d**esorption branch)

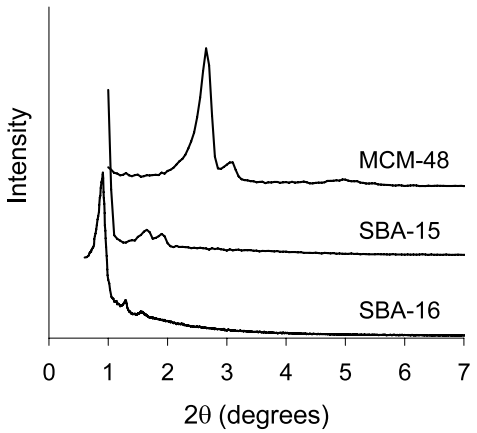

Fig. 2 X-ray diffraction patterns for the merged SBA-15, SBA-16 and MCM-48 samples used in liquid adsorption experiments

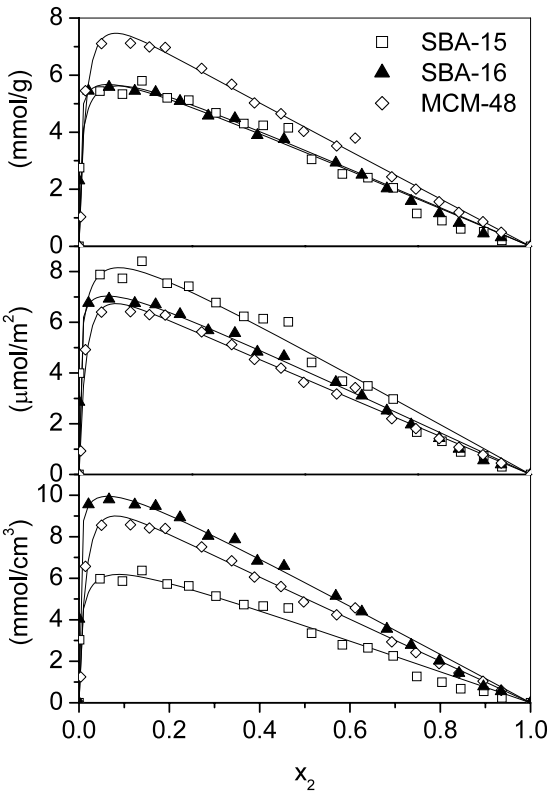

Fig. 3 Specific, areal and volume $\Gamma_2^{(n)}$ adsorption excesses of ethanol(2) from n-octane(1)/ethanol(2) on SBA-15, SBA-16 and MCM-48 at 25 °C

mesopore size distributions and known from literature. The textural data of the adsorbents calculated from the isotherms are listed in Table 1. Figure 2 shows the powder X-ray diffraction patterns of the merged SBA-15, SBA-16 and MCM-48 samples with diffraction peaks being characteristic of the SBA-15 hexagonal $p\bar{6}mm$, the SBA-16 cubic $Im\bar{3}m$ and the MCM-48 cubic $Ia\bar{3}d$ symmetry.

In the following, experimental liquid-adsorption data at 25 °C will be presented. The discussion will be based on adsorption excess isotherms given in Figs. 3–6. The adsorption excess data are listed in Tables 2–4, the Bi-Langmuir parameters of the corresponding isotherms (solid lines in Figs. 3–6) are given in Table 5.

Figure 3 illustrates the experimental $\Gamma_2^{(n)}$ adsorption excesses of n-octane(1)/ethanol(2) on SBA-15, SBA-16 and MCM-48 with about 20 data points over the whole concentration range. The specific $\Gamma_2^{(n)}$ excess isotherm points in mmol/g (cf. the top diagram of Fig. 3) are converted into areal adsorption excesses in μ mol/m^2 (the middle diagram of Fig. 3) and volume adsorption excesses in mmol/cm^3 (the bottom diagram of Fig. 3) by means of the BET specific surface areas and total pore volumes of the silicas given in Table 1. As can be seen, all isotherms correspond to type II of the classification according to Schay and Nagy. Ethanol is preferentially adsorbed from the binary mixture over the whole concentration range. Such adsorption behavior is typical for systems with a mixture of both a non-polar and a polar component adsorbed on a polar solid surface. The strong rise of the isotherms in the small mole fraction range of ethanol refers to the selectivity of the silica surfaces for polar components. However, the magnitude of adsorption excesses is remarkable. The highest specific adsorption excess is found for MCM-48 with more than 7 mmol/g at $x_2 \approx 0.1$, whereas the specific adsorption excesses of SBA-15 and SBA-16 are comparable (about 5.5 mmol/g at $x_2 \approx 0.1$). For the areal adsorption excess presented in the middle diagram of Fig. 3, an inversion can be found. As a result of the large BET specific surface area of MCM-48 (cf. Table 1), the areal

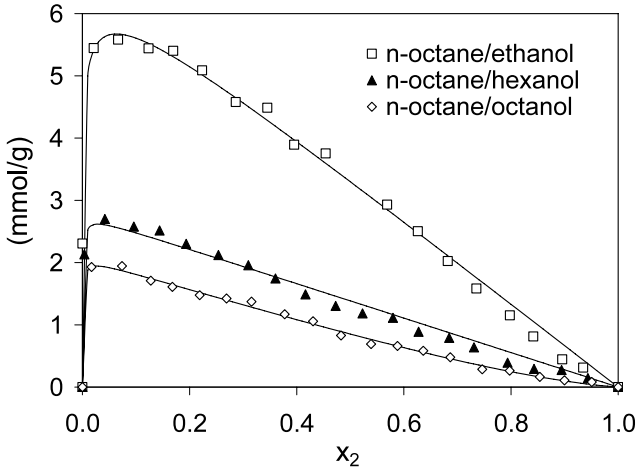

Fig. 4 Specific $\Gamma_2^{(n)}$ adsorption excesses of alcohol(2) from n-octane(1)/alcohol(2) mixtures on SBA-16 at 25 °C

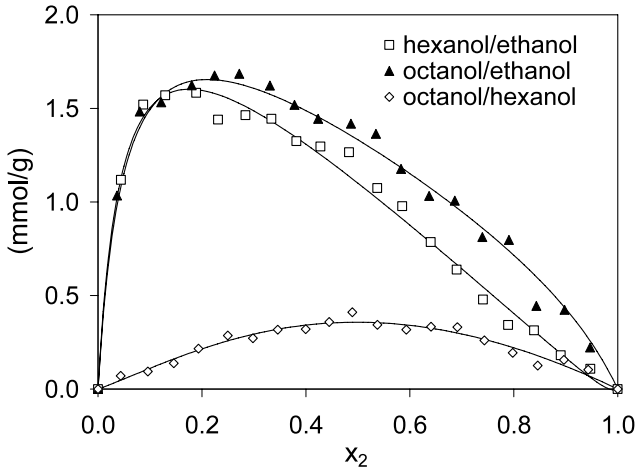

Fig. 5 Specific $\Gamma_2^{(n)}$ adsorption excess of alcohol(2) from alcohol(1)/alcohol(2) mixtures on SBA-16 at 25 °C

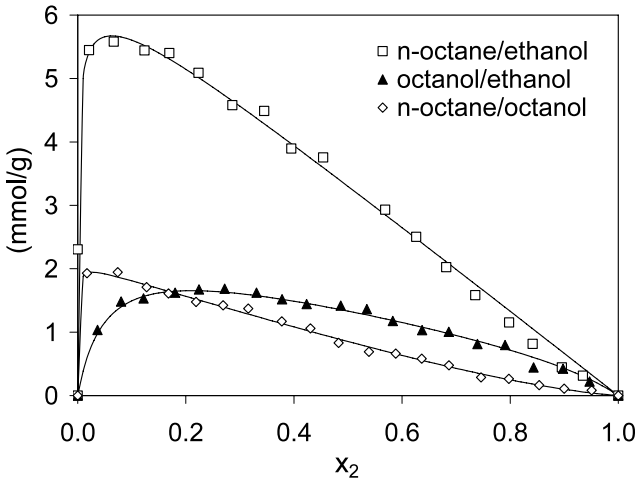

Fig. 6 Specific $\Gamma_2^{(n)}$ adsorption excesses of ethanol(2) and octanol(2) from n-octane(1)/ethanol(2), n-octane(1)/octanol(2) and octanol(1)/ethanol(2) on SBA-16 at 25 °C

adsorption excess for MCM-48 is the smallest and that for SBA-15 the highest one. A second inversion can be found for the volume adsorption excesses (see the bottom diagram of Fig. 3) as a result of the high SBA-15 total pore volume (cf. Table 1).

For interpreting Fig. 3 one should consider that at first view liquid adsorption isotherms grant only integral information representing liquid as well as solid qualities. As the liquid mixture is identical, the differences in isotherms should be attributed to the structural and energetical parameters of the solids. With regard to solid parameters, however, the smaller areal adsorption excess on MCM-48 compared to that on SBA-15 can be caused either by a smaller polarity of the MCM-48 surface or by structural effects such as the smaller MCM-48 mesopore size of 2 nm—taking into consideration that molecular state and orientation of ethanol and n-octane in the interfacial region are unknown. Since SBA-15 and SCA-16 contain in addition a considerable amount of micropores, it has to be said that present phenomenological information is too small to extract the influence of mesopore size or structure on the isotherms.

Figures 4–6 show the adsorption excesses of different binary liquid mixtures on SBA-16 (cf. Figs. 1 and 2), i.e., not the solid adsorbent, as in the previous case, is varied, but the liquid mixtures. In Fig. 4, the specific adsorption excesses of three n-octane/alcohol mixtures on SBA-16 are presented. In each case, the alcohol component is preferentially adsorbed from the binary mixture. The preferential adsorption decreases with increasing chain length of the alcohol molecule, i.e., the adsorption excesses decrease in the row ethanol-hexanol-octanol. This result is not surprising if one considers that the polarity of the alcohol molecules and therefore the difference to the non-polar n-octane molecule diminishes with increasing chain length. Looking at the three regular isotherms, it even seems that the pure influence of single carbon groups (CH_2/CH_3) and the OH group of the alcohols can be separated. n-Octane and ethanol differ in 6 carbon groups and the OH group causing a strong preferential adsorption of ethanol, n-octane and hexanol differ in 2 carbon groups and the OH group causing a weaker preferential adsorption of hexanol, and n-octane and octanol differ only in the OH group causing the weakest preferential adsorption of octanol and showing the pure influence of the OH group.

The influence of the chain length of adsorptive molecules can also be studied regarding the specific adsorption excesses of three alcohol/alcohol mixtures on SBA-16 (see Fig. 5). In each case, the alcohol with the smaller chain length is preferentially adsorbed from binary mixture. The highest adsorption excess is found for ethanol from the octanol/ethanol mixture (6 carbon groups difference), a smaller one for ethanol from hexanol/ethanol (4 carbon groups difference) and the smallest one for octanol/hexanol

Table 2 Experimental specific adsorption excesses of n-octane(1)/ethanol(2) on SBA-15, SBA-16 and MCM-48 at 25 °C

SBA-15		SBA-16		MCM-48	
x_2	$\Gamma_2^{(n)}$ (mmol/g)	x_2	$\Gamma_2^{(n)}$ (mmol/g)	x_2	$\Gamma_2^{(n)}$ (mmol/g)
1	0	1	0	1	0
0.9366	0.21	0.9346	0.31	0.9351	0.50
0.8964	0.51	0.8956	0.44	0.8946	0.86
0.8454	0.61	0.8416	0.81	0.8413	1.19
0.8037	0.90	0.7980	1.15	0.7973	1.57
0.7480	1.15	0.7355	1.58	0.7459	2.01
0.6958	2.05	0.6818	2.02	0.6926	2.44
0.6399	2.41	0.6262	2.50	0.6117	3.40
0.5832	2.54	0.5687	2.93	0.5706	3.52
0.5152	3.05	0.4540	3.75	0.4975	4.03
0.4637	4.15	0.3951	3.89	0.4470	4.65
0.4079	4.24	0.3451	4.49	0.3883	5.03
0.3650	4.30	0.2861	4.58	0.3379	5.68
0.3032	4.68	0.2235	5.09	0.2714	6.23
0.2431	5.12	0.1695	5.40	0.1908	6.97
0.1953	5.20	0.1235	5.44	0.1557	6.99
0.1393	5.80	0.0666	5.58	0.1139	7.12
0.0961	5.34	0.0210	5.45	0.0498	7.10
0.0465	5.44	0.0001	2.31	0.0141	5.46
0.0011	2.76	0	0	0.0037	1.03
0	0			0	0

Table 3 Experimental specific adsorption excesses of three n-octane(1)/alcohol(2) mixtures on SBA-16 at 25 °C

n-octane(1)/ethanol(2)		n-octane(1)/hexanol(2)		n-octane(1)/octanol(2)	
x_2	$\Gamma_2^{(n)}$ (mmol/g)	x_2	$\Gamma_2^{(n)}$ (mmol/g)	x_2	$\Gamma_2^{(n)}$ (mmol/g)
1	0	1	0	1	0
0.9346	0.31	0.9434	0.14	0.9506	0.08
0.8956	0.44	0.8944	0.27	0.8997	0.11
0.8416	0.81	0.8429	0.29	0.8536	0.16
0.7980	1.15	0.7936	0.39	0.7975	0.26
0.7355	1.58	0.7307	0.64	0.7461	0.29
0.6818	2.02	0.6844	0.79	0.6866	0.48
0.6262	2.50	0.6273	0.89	0.6362	0.58
0.5687	2.93	0.5795	1.11	0.5881	0.66
0.4540	3.75	0.5227	1.18	0.5387	0.69
0.3951	3.89	0.4726	1.30	0.4826	0.83
0.3451	4.49	0.4162	1.49	0.4305	1.06
0.2861	4.58	0.3602	1.74	0.3775	1.17
0.2235	5.09	0.3095	1.96	0.3155	1.37
0.1695	5.40	0.2539	2.12	0.2690	1.42
0.1235	5.44	0.1937	2.30	0.2189	1.48
0.0666	5.58	0.1441	2.52	0.1680	1.61
0.0210	5.45	0.0960	2.58	0.1275	1.71
0.0001	2.31	0.0418	2.70	0.0739	1.94
0	0	0.0035	2.13	0.0171	1.93
		0	0	0	0

Table 4 Experimental specific adsorption excesses of three alcohol(1)/alcohol(2) mixtures on SBA-16 at 25 °C

Octanol(1)/hexanol(2)		Hexanol(1)/ethanol(2)		Octanol(1)/ethanol(2)	
x_2	$\Gamma_2^{(n)}$ (mmol/g)	x_2	$\Gamma_2^{(n)}$ (mmol/g)	x_2	$\Gamma_2^{(n)}$ (mmol/g)
1	0	1	0	1	0
0.9430	0.10	0.9474	0.11	0.9467	0.22
0.8964	0.16	0.8903	0.18	0.8977	0.42
0.8460	0.13	0.8388	0.31	0.8433	0.44
0.7979	0.19	0.7890	0.34	0.7906	0.80
0.7433	0.26	0.7408	0.48	0.7393	0.81
0.6912	0.33	0.6899	0.64	0.6864	1.01
0.6406	0.33	0.6401	0.79	0.6371	1.03
0.5931	0.32	0.5853	0.98	0.5829	1.18
0.5374	0.34	0.5372	1.07	0.5347	1.36
0.4893	0.41	0.4831	1.27	0.4865	1.42
0.4448	0.36	0.4280	1.30	0.4234	1.44
0.3995	0.32	0.3816	1.32	0.3781	1.52
0.3458	0.32	0.3335	1.44	0.3307	1.62
0.2981	0.27	0.2837	1.46	0.2718	1.68
0.2497	0.29	0.2310	1.44	0.2242	1.68
0.1933	0.22	0.1889	1.58	0.1803	1.62
0.1457	0.14	0.1293	1.57	0.1217	1.53
0.0959	0.09	0.0870	1.52	0.0803	1.48
0.0436	0.07	0.0442	1.12	0.0366	1.03
0	0	0	0	0	0

Table 5 Bi-Langmuir parameters of (2) for the experimental specific adsorption excess isotherms at 25 °C

Liquid mixture	Solid	Γ_2^s	h_1	U_1	U_2	SMSE[1]
n-octane/ethanol	MCM-48	8.2293	6.9063	8.8375	8.3344	1.97
n-octane/ethanol	SBA-15	6.8830	0.3891	24.2510	10.0049	1.47
n-octane/ethanol	SBA-16	6.7343	0.8287	16.2322	7.1634	0.32
n-octane/hexanol	SBA-16	2.7743	−3.2462	25.1436	20.7817	0.21
n-octane/octanol	SBA-16	2.8736	0.7254	17.1980	−2.5673	0.03
hexanol/ethanol	SBA-16	2.6286	0.9617	7.5293	−9.2029	0.07
octanol/ethanol	SBA-16	1.9060	1.2991	7.3559	−4.8711	0.03
octanol/hexanol	SBA-16	4.1321	1.5940	1.3982	2.3806	0.01

[1] Sum of mean squared errors

(2 carbon groups difference). As can be clearly seen, the influence of the chain length is not linear. Whereas the preferential adsorption of hexanol from octanol/hexanol is very weak, ethanol is noticeably preferentially adsorbed from hexanol (as well as from octanol), and the isotherm maximum is shifted to smaller mole fractions. The experimental adsorption excesses indicate that the importance of the chain-length difference on the adsorption diminishes with increasing chain length of the components of a binary mixture. This conclusion is also supported by the small quantitative difference in the n-octane/hexanol and n-octane/octanol isotherms in Fig. 4.

Beside the ternary octanol/hexanol/ethanol/SBA-16 adsorption system given in Fig. 5, three further ternary adsorption systems can be constructed by means of the binary adsorption data presented in Figs. 3–5:

- the n-octane/octanol/hexanol/SBA-16 system
- the n-octane/octanol/ethanol/SBA-16 system
- the n-octane/hexanol/ethanol/SBA-16 system.

For the purpose of illustration, we will show in Fig. 6 the adsorption excesses of n-octane/octanol, n-octane/ethanol and octanol/ethanol on SBA-16, i.e., the binary random isotherms of the ternary n-octane/octanol/ethanol/SBA-16 system. Whereas the n-octane/alcohol isotherms are type II isotherms (with a strong preferential adsorption of the short-chain ethanol molecule from the n-octane/ethanol mixture, cf. Fig. 4), the octanol/ethanol isotherm corresponds rather

to type I of the Schay and Nagy classification (cf. Fig. 5). A successful consistency test (Kalies and Bräuer 2005) of the measured binary adsorption data was carried out, i.e., the presented binary adsorption data can be used as basis for the thermodynamic treatment outlined in the introduction.

5 Conclusions

The work is a first step to create a data base of liquid-phase adsorption on solids with ordered mesopore structure. The adsorption excesses at 25 °C of the following completely miscible, binary liquid mixtures on silicas with ordered mesopore structure were presented:

- n-octane/ethanol/MCM-48
- n-octane/ethanol/SBA-15
- n-octane/ethanol/SBA-16
- n-octane/hexanol/SBA-16
- n-octane/octanol/SBA-16
- octanol/hexanol/SBA-16
- octanol/ethanol/SBA-16
- hexanol/ethanol/SBA-16.

The measured isotherms were discussed with regard to the structural parameters of the solids, the separation quality of the solid and the dependence on the chain length of adsorptive molecules. The silicas are highly selective for polar components and should find, once a low-cost and large-scale synthesis can be performed, application in separation and cleaning processes. The binary data are consistent and allow thermodynamic calculations such as the determination of separation diagrams and the construction of the following ternary adsorption systems:

- n-octane/octanol/hexanol/SBA-16
- n-octane/octanol/ethanol/SBA-16
- n-octane/hexanol/ethanol/SBA-16
- octanol/hexanol/ethanol/SBA-16.

In this way, the data bank of complete tabular sets of binary liquid adsorption isotherms for creating ternary ones is extended.

Acknowledgement The financial support for this project by Deutsche Forschungsgemeinschaft (DFG, Ka 1560/2-1, 2-3) is gratefully acknowledged.

References

Bräuer, P., Heuchel, M., Jaroniec, M.: Thermodynamic description of interfaces. In: Encyclopedia of Surface and Colloid Science, pp. 5326–5343. Dekker, New York (2002)

Choi, M., Heo, W., Kleitz, F., Ryoo, R.: Facile synthesis of high quality mesoporous SBA-15 with enhanced control of the porous network connectivity and wall thickness. Chem. Commun., 1340–1341 (2003)

Everett, D.H.: Reporting data on adsorption from solution at the solid/solution interface. Pure Appl. Chem. **58**, 967–984 (1986)

Heuchel, M., Bräuer, P., Szombately, M.V., Messow, U., Einicke, W.-D., Jaroniec, M.: Evaluation of the energy distribution function from liquid/solid adsorption measurements. Langmuir **9**, 2547–2554 (1993)

IUPAC International Union of Pure and Applied Chemistry: Quantities, Units and Symbols in Physical Chemistry, 2nd edn., pp. 64. Blackwell, Cambridge (1993)

Kalies, G., Bräuer, P.: Application of excess formalism to multicomponent liquid adsorption equilibria. Adsorption **11**, 229–234 (2005)

Kalies, G., Bräuer, P., Messow, U., Kärger, J.: Calculation of separation diagrams from ternary liquid adsorption on carbonaceous adsorbents. Sep. Purif. Technol. **20**, 41–48 (2000a)

Kalies, G., Bräuer, P., Rouquérol, F.: Prediction of ternary liquid adsorption on solids from binary data. J. Colloid Interface Sci. **229**, 407–417 (2000b)

Kalies, G., Rockmann, R., Denoyel, R.: Calculation of immersion enthalpy data from adsorption excess isotherms. J. Colloid Interface Sci. **282**, 327–334 (2005)

Kim, T.W., Ryoo, R., Gierszal, K.P., Jaroniec, M., Solovyov, L.A., Sakamoto, Y., Terasaki, O.: Characterization of mesoporous carbons synthesized with SBA-16 silica template. J. Mater. Chem. **15**, 1560–1571 (2005)

Kleitz, F., Kim, T.E., Ryoo, R.: Design of mesoporous silica at low acid concentrations in triblock copolymer-butanol-water systems. Bull. Korean Chem. Soc. **26**, 1653–1668 (2005)

Kruk, M., Jaroniec, M., Ko, C.H., Ryoo, R.: Characterization of the porous structure of SBA-15. Chem. Mater. **12**, 1961–1968 (2000)

Myers, A.L., Price, P.E., Danner, R.P.: Letters to the editor. AIChE J. **33**, 1757 (1987)

Price, P.E., Danner, R.P.: Prediction of multicomponent liquid adsorption equilibria. AIChE J. **33**, 551–557 (1987)

Rockmann, R., Kalies, G.: Characterization and adsorptive application of ordered mesoporous silicas. Appl. Surf. Sci. **253**, 5666–5670 (2007)

Sorensen, O.T., Rouquérol, J.: Sample Controlled Thermal Analysis. Kluwer, Dordrecht (2003)

Thommes, M.: Physical adsorption characterization of ordered and amorphous mesoporous materials. In: Lu, G.Q., Zhao, X.X. (Eds.) Nanoporous Materials: Science and Engineering, pp. 317–364. Imperial College Press (2004)

Wang, S., Wu, D., Sun, Y., Zhong, B.: The synthesis of MCM-48 with high yields. Mater. Res. Bull. **36**, 1717–1720 (2001)

Zhao, D., Feng, J., Huo, Q., Melosh, N., Fredrickson, G.H., Chmelka, B.F., Stucky, G.D.: Triblock copolymer syntheses of mesoporous silica with periodic 50 to 300 Angstrom pores. Science **279**, 548–552 (1998a)

Zhao, D., Huo, Q., Feng, J., Chmelka, B.F., Stucky, G.D.: Nonionic triblock and star diblock copolymer and oligomeric surfactant syntheses of highly ordered, hydrothermally stable, mesoporous silica structures. J. Am. Chem. Soc. **120**, 6024–6036 (1998b)